

Electrodes Properties of Prussian Blue Analogues

Yutaka Moritomo^{1,2}, Masamitsu Takachi¹, Yutaro Kurihara¹

¹School of Science and Engineering, University of Tsukuba, Tsukuba, Ibaraki 305-8571, Japan

²TIMS, University of Tsukuba, Tsukuba305-8571, Japan

1 Introduction

Recently, Matsuda and Moritomo [1] reported that a thin film of the Prussian blue analogue, $\text{Na}_{1.32}\text{Mn}[\text{Fe}(\text{CN})_6]_{0.83}3.5\text{H}_2\text{O}$ exhibits a large capacity (=128 mAh/g) and good cyclability (=87% of the initial value at 100 cycles). The Prussian blue analogues, represented as $\text{A}_x\text{M}[\text{Fe}(\text{CN})_6]_y\text{zH}_2\text{O}$ (A and M are an alkali metal and a transition metal, respectively.), form a three-dimensional (3D) network structure (-M-NC-Fe-CN-M-) The alkali cations (At) and some water molecules (zeolite waters) occupy the nanopores of the framework, while the remaining water molecules (ligand waters) occupy the vacancy of the $\text{Fe}(\text{CN})_6$ unit and coordinate to M. Importantly, the framework is robust against the Li^+ insertion/extraction process, reflecting the strong p-d hybridization between Fe and C. However, there are few reports on the electronic and crystal structures of the Li-substituted Prussian blue analogues. also the discharge voltage in the plateau region.

2 Experiment

Thin films of $\text{Na}_{0.72}\text{Ni}[\text{Fe}(\text{CN})_6]_{0.68}5.1\text{H}_2\text{O}$ (denoted as NNF68), $\text{Na}_{0.84}\text{Co}[\text{Fe}(\text{CN})_6]_{0.71}3.8\text{H}_2\text{O}$ (NCF71), $\text{Na}_{1.24}\text{Mn}[\text{Fe}(\text{CN})_6]_{0.81}3.0\text{H}_2\text{O}$ (NMF81), and $\text{Na}_{1.84}\text{Cd}[\text{Fe}(\text{CN})_6]_{0.96}4.8\text{H}_2\text{O}$ (NCdF96) were electrochemically synthesized on an indium tin oxide (ITO) transparent electrode under potentiostatic conditions at 0:50V vs a Ag/AgCl electrode in an aqueous solution. The thicknesses of the films were 1 μm , which were measured with a profilometer (Dektak3030). The mass of each film was measured with a conventional electronic weighing machine after the film was carefully removed from the ITO glass with a microspatula. The experimental error of the mass is $\pm 10\%$. Chemical compositions of the films were determined by the inductively coupled plasma (ICP) method and CHN organic elementary analysis (Perkin-Elmer 2400 CHN Elemental Analyzer). Rietveld analysis of the XRD pattern revealed that the compounds are fcc with lattice constant: $a = 10.200(3)\text{Å}$ for NNF68, $10.296(2)\text{Å}$ for NCF71, $10.544(2)\text{Å}$ for NMF81, and $10.7001(4)\text{Å}$ for NCdF96.

The Li^+ was substituted for Na by performing charge/discharge cycles of the thin films against Li. The electrolyte was ethylene carbonate (EC)/diethyl carbonate (DEC) solution containing 1 mol/L LiClO_4 . The charge/discharge current is 10 μA , and the cutoff voltage was from 2.0 to 4.2 V. Thus, we obtained thin film electrodes, i.e., $\text{Li}_x\text{Na}_{0.04}\text{Ni}[\text{Fe}(\text{CN})_6]_{0.68}5.1\text{H}_2\text{O}$ (M = Ni),

$\text{Li}_x\text{Na}_{0.13}\text{Co}[\text{Fe}(\text{CN})_6]_{0.71}3.8\text{H}_2\text{O}$ (M = Co), $\text{Li}_x\text{Mn}[\text{Fe}(\text{CN})_6]_{0.81}3.0\text{H}_2\text{O}$ (M = Mn), and $\text{Li}_x\text{Na}_{0.88}\text{Cd}[\text{Fe}(\text{CN})_6]_{0.96}4.8\text{H}_2\text{O}$ (M = Cd). In the XRD and XAFS experiments, the Li concentration (x) was controlled by the cutoff voltage.

3 Results and Discussion

Figure 1 shows the discharge curves of thin-film electrodes at various rates (v). The area of each thin-film electrode was 1–2 cm^2 . The electrolyte and the cutoff voltage are the same as above. The discharge curve at v was measured after the charge process at v . The discharge capacities at small v coincide with the ideal value within the experimental error (= 10%). In all the compounds, the curves show plateaus at 3:5V due to the reduction of Fe (vide infra). The plateau behavior is observed even at large v . At large v , however, the discharge voltage was slightly suppressed due to the battery resistance. The capacities at 100 C are 66% (Ni), 31% (Co), 62% (Mn), and 74% (Cd) of those at 1C.

Figure 2 shows the XAFS spectra of the thin film electrodes against x. The measurements were carried out at the 7C beamline of Photon Factory (PF), KEK. The XAFS spectra near the Fe K-edge, Ni K-edge, Co K-edge, Mn K-edge, and Cd L1-edge were recorded by a Lytle detector in fluorescent yield mode with a Si(111) double-crystal monochromator and were normalized by the intensities at 7140, 8360, 7740, 6560, and 4060 eV, respectively. In all the compounds, the absorption peaks in the Fe K-edge spectra [Figs. 2(a), 2(c), 2(e), and 2(g)] show a redshift with increasing in x. The redshift is ascribed to the reduction of Fe (low-spin $\text{Fe}^{3+} \rightarrow$ low-spin Fe^{2+}). On the other hand, the absorption peaks in the Ni K-edge (b), Co K-edge (d), Mn K-edge (f), and Cd L1-edge (h) spectra show no shift, indicating that the valence states of M remain unchanged.

Figure 3 shows lattice constants (a) against x. the lattice constants were refined by the Rietveld method (Rietan-FP). Except for the Cd compound, a slightly decreases with increasing in x. The decrease in a is probably due to the smaller size of $[\text{Fe}(\text{CN})_6]^{4-}$ than that of $[\text{Fe}(\text{CN})_6]^{3-}$. Actually, the $\text{Fe}^{\text{II}}\text{-N}$ bond length (=3.00–3.01 Å) is shorter than the $\text{Fe}^{\text{III}}\text{-N}$ bond length (=3.10 Å) in $\text{RbMn}[\text{Fe}(\text{CN})_6]$.

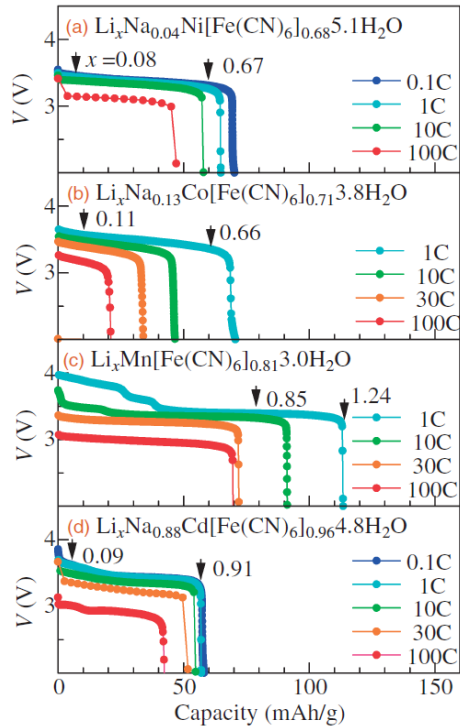


Fig. 1: Discharge curves of thin-film electrodes of (a) $\text{Li}_x\text{Na}_{0.04}\text{Ni}[\text{Fe}(\text{CN})_6]_{0.68}5.1\text{H}_2\text{O}$, (b) $\text{Li}_x\text{Na}_{0.13}\text{Co}[\text{Fe}(\text{CN})_6]_{0.71}3.8\text{H}_2\text{O}$, (c) $\text{Li}_x\text{Mn}[\text{Fe}(\text{CN})_6]_{0.81}3.0\text{H}_2\text{O}$, and (d) $\text{Li}_x\text{Na}_{0.88}\text{Cd}[\text{Fe}(\text{CN})_6]_{0.96}4.8\text{H}_2\text{O}$ against Li at various rates.

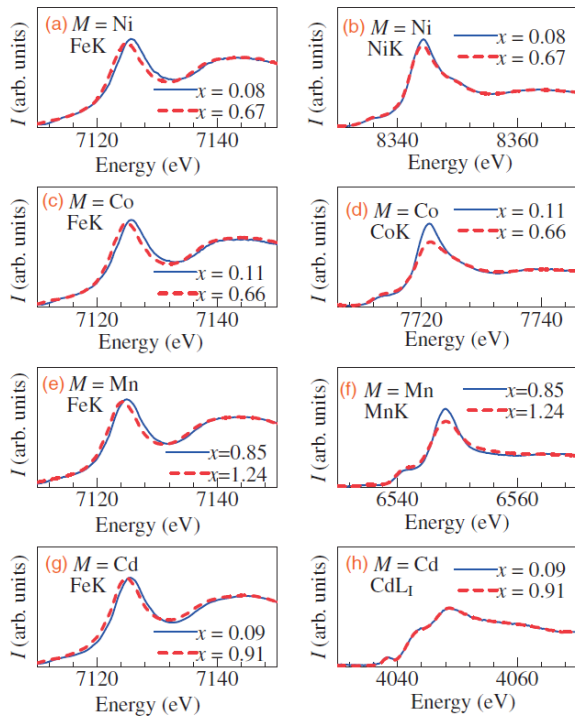


Fig. 2: X-ray absorption spectra of (a,b) $\text{Li}_x\text{Na}_{0.04}\text{Ni}[\text{Fe}(\text{CN})_6]_{0.68}5.1\text{H}_2\text{O}$, (c,d) $\text{Li}_x\text{Na}_{0.13}\text{Co}[\text{Fe}(\text{CN})_6]_{0.71}3.8\text{H}_2\text{O}$, (e,f) $\text{Li}_x\text{Mn}[\text{Fe}(\text{CN})_6]_{0.81}3.0\text{H}_2\text{O}$, and (g,h) $\text{Li}_x\text{Na}_{0.04}\text{Ni}[\text{Fe}(\text{CN})_6]_{0.68}5.1\text{H}_2\text{O}$ against x .

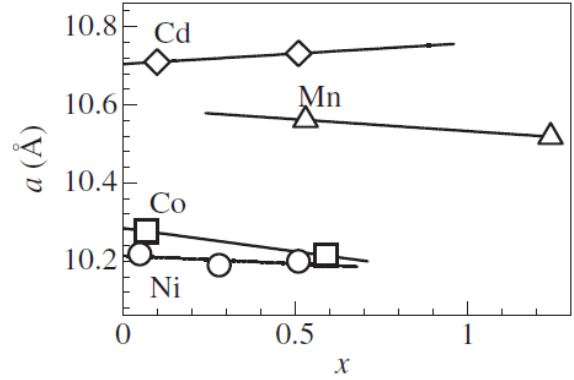


Fig. 3: Lattice constant (a) of (a) $\text{Li}_x\text{Na}_{0.04}\text{Ni}[\text{Fe}(\text{CN})_6]_{0.68}5.1\text{H}_2\text{O}$, (b) $\text{Li}_x\text{Na}_{0.13}\text{Co}[\text{Fe}(\text{CN})_6]_{0.71}3.8\text{H}_2\text{O}$, (c) $\text{Li}_x\text{Mn}[\text{Fe}(\text{CN})_6]_{0.81}3.0\text{H}_2\text{O}$, and (d) $\text{Li}_x\text{Na}_{0.88}\text{Cd}[\text{Fe}(\text{CN})_6]_{0.96}4.8\text{H}_2\text{O}$ against x . Straight lines are results of the least-squares fitting, and also represent the Fe redox region.

Acknowledgement

This work was supported by a Grant-in-Aid for Scientific Research (No. 21244052) from the Ministry of Education, Culture, Sports, Science and Technology, Japan. The X-ray powder diffraction and X-ray absorption experiments were performed under the approval of the Photon Factory Program Advisory Committee (Proposal Nos. 2010G502, 2011G501, 2013G501, and 2013G068). The elementary analysis of the films was performed at the Chemical Analysis Division, Research Facility Center for Science and Engineering, University of Tsukuba.

References

[1] T. Matsuda and Y. Moritomo: *Appl. Phys. Express* **4** 047101 (2011).

* moritomo.yutaka.gf@u.tsukuba.ac.jp